Available online at www.sciencedirect.com
SCIENCE DIRECT®
Journal of Solid State Chemistry 177 (2004) 1312–1320
JOURNAL OF SOLID STATE CHEMISTRY
http://elsevier.com/locate/jssc

Rare earth phosphate powders $RePO_4 \cdot nH_2O$ (Re = La, Ce or Y) II. Thermal behavior

S. Lucas,[a] E. Champion,[a,*] D. Bernache-Assollant,[a] and G. Leroy[b]

[a] *Science des Procédés Céramiques et de Traitements de Surface, Université de Limoges, UMR CNRS 6638, 123, Avenue Albert Thomas, 87060 Limoges Cedex, France*

[b] *Laboratoire de Biomatériaux, Faculté de Chirurgie Dentaire, Place de Verdun, 59000 Lille, France*

Received 22 July 2003; received in revised form 30 October 2003; accepted 6 November 2003

Abstract

The thermal behavior, thermostructural and morphological changes, of rare earth phosphate powders $RePO_4 \cdot nH_2O$ (Re = La, Ce or Y) was investigated up to 1500°C using high temperature X-ray diffraction, FT-infrared and Raman spectroscopies and thermogravimetry coupled with differential thermal analysis. The hydration water of the compounds was zeolitic (for Re = La or Ce) or coordinated (for Re = Y) and was associated with a divariant or a monovariant equilibrium of dehydration, respectively. The high temperature anhydrous monoclinic phase $LaPO_4$ or $CePO_4$ formed irreversibly at about 750°C after the total dehydration of the hexagonal hydrated structure while the dehydration of the monoclinic $YPO_4 \cdot 2H_2O$ phase began from about 190°C with its simultaneous decomposition into tetragonal YPO_4. A polytrioxophosphate secondary minor phase $Re(PO_3)_3$ resulting from adsorbed H_3PO_4 was formed at 950°C and decomposed at 1350°C. The particle morphology did not change with the temperature but grain coalescence occurred below 1000°C.

Keywords: Rare earth phosphate; Thermal behavior; Rhabdophane; Churchite; Monazite; Xenotime; Polytrioxophosphate

1. Introduction

This paper is the second part of a study devoted to rare earth phosphate compounds. It concerns the thermal behavior of three rare earth phosphate powders (Re = La, Ce or Y), the synthesis of which was exposed in part I [1]. Several authors have investigated the thermal behavior of rare earth phosphates in order to determine the temperatures of thermostructural changes from the hydrated to the anhydrous phosphate forms for the different lanthanide ions based compounds [2–6]. Hikichi et al measured the melting point of the main lanthanide phosphates $LnPO_4$ [7]. At the end of the 1970s, some works have been devoted to the formation of new compounds from the decomposition of rare earth phosphates at high temperature [8–10]. Then, studies concerning the establishment of phase diagrams in the system Ln_2O_3–P_2O_5 were published for Ln = La [11, 12], Nd [13] or Ln = Y and Gd [14]. But, there is no study dealing with the high temperature behavior of synthetic rare earth phosphate powders from a more global approach with the aim of elaborating dense ceramic parts. The knowledge of the behavior of powders at high temperature is of prime importance in order to control the sintering, and therefore the properties of the densified ceramic materials.

The aim of this work was thus to determine the structural and morphological changes of lanthanum, cerium or yttrium phosphate powders according to the temperature as well as the domains of thermal stability of the different phases. To this end, thermogravimetry coupled with differential thermal analysis, high temperature X-ray diffraction, Fourier transform infrared spectroscopy and Raman spectroscopy were used.

2. Materials and methods

The powders were prepared from the aqueous precipitation method detailed in part I of the study. For the present part of the work, the syntheses were

*Corresponding author. Fax: +33-5-55-45-75-86.
E-mail address: champion@unilim.fr (E. Champion).

0022-4596/$ - see front matter © 2003 Elsevier Inc. All rights reserved.
doi:10.1016/j.jssc.2003.11.004

Table 1
Main characteristics of the raw precipitates

Reference	LaP Tamb	LaP T50h20	CeP T50h20	YP T50h00	YP T50h01
Structure	Hexagonal	Hexagonal	Hexagonal	Amorphous	Monoclinic
(PDF file No.)	46–1439	46–1439	35–614		85–1842
Hydration H_2O/mol	0.61	0.57	0.60	1.2	2
$S_0/m^2\,g^{-1}$	78.4±0.4	68.8±0.3	69±1.0	105±1.0	1.95±0.03
Bulk density	3.90	3.98	4.16	2.95	2.18
Re/P					
Mole ratio	0.90	0.94	0.96	0.93	0.95
$Re(PO_3)_3$					
(wt%)	2.18	1.62	1.11	1.40	0.80

performed using a *Re*/P mole ratio of the initial reagents equal to 1 without any control of the pH value, at different temperatures (referred as *Txx*, with *xx* in Celsius degree) and for various ripening times (referred as *hyy*, with *yy* in hours). The main characteristics of these powders are summarized in Table 1. Lanthanum or cerium phosphate powders were rhabdophane-type compounds (hexagonal system) while yttrium phosphate powders were either amorphous or churchite-type compound (monoclinic system). Elementary analyses, X-ray diffraction (XRD), Fourier-transform infrared spectrometry (FTIR), scanning electron microscopy (SEM), specific surface area measurements (S_0) and bulk density measurements were performed according to the procedures already described in part I.

Raman spectra were obtained with helium–neon laser excitation (632.8 nm) using an OMARS 89 spectrometer coupled with a metallographic microscope. The spectra were recorded in the 170–3700 cm^{-1} range with a resolution of 2 cm^{-1}.

The thermostructural evolution of powders was investigated from high temperature X-ray diffraction (XRD) using a diffractometer (Siemens, Model D5000, Germany) fitted out with a high temperature furnace (Anton Paar HTK 10, Pt heating sample holder) and an Elphyse position detector (aperture: 14°). The heating rate was 10°C min^{-1}. Each diagram was recorded after a setting time of 10 min at the chosen temperature in the range 20–1100°C under air atmosphere.

Thermogravimetric analysis (TGA) of powders coupled with differential thermal analysis (DTA) was performed up to 1500°C at the heating rate of 10°C min^{-1} under nitrogen gas flow (TA instruments, model SDT 2960, USA). For these analyses, powder samples were put in a Pt crucible. Dilatometry measurements were made using a Setaram equipment (model TMA 92, France). The heating rate was 5°C min^{-1}. The powder was initially pressed in a 10 mm diameter die at 120 MPa to produce cylindrical samples with a compaction ratio of about 60%. The linear shrinkage (or expansion) was measured using an alumina extensometer. The contact load between the extensometer and the sample was 5.10^{-2} N.

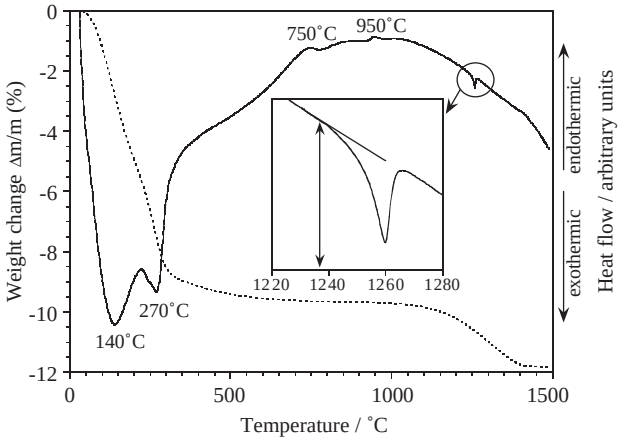

Fig. 1. TGA (dashed line) and DTA of lanthanum phosphate precipitate LaP Tamb.

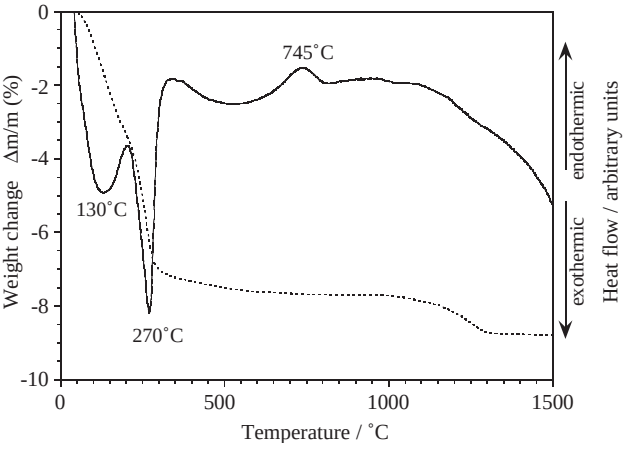

Fig. 2. TGA (dashed line) and DTA of cerium phosphate precipitate CeP T50h20.

3. Results and discussion

3.1. Lanthanum and cerium phosphates

Typical TGA and DTA plots of lanthanum and cerium phosphate powders are given in Figs. 1 and 2, respectively. Similar behavior was observed, the weight

loss occurring in three steps. The first one, below 200°C, was associated with the release of 3–4 wt% of residual water adsorbed on the powder surface due to the storage conditions in air (raw precipitates were dried at 80°C for 24 h after synthesis, then stocked. But they were not dried again before TG experiments). It was accompanied by an endothermic effect whose maximum was at about 130–140°C. The second began at about 200°C and finished at about 600°C. It corresponded with the dehydration of the hydrated hexagonal $RePO_4 \cdot nH_2O$ phase (rhabdophane-type). This step proceeded in two sequences. An important weight loss was registered between 200°C and 300°C. Then, the dehydration decreased slowly up to 600°C. Each sequence is accompanied by an endothermic effect. The first one was a marked peak with a maximum at 270°C and the second was much broader. The total weight loss measured during this second step depended on the synthesis conditions and corresponded to a hydration ratio n of the compound between 0.5 and 0.65 mole. Above 600°C two exothermic peaks appeared and were not associated with any detectable weight change. The first one began at 600°C with a maximum at 750°C while the second occurred at 950°C (Fig. 1). Then, at higher temperature a third weight loss, which was not expected to occur on the hypothesis of pure rare earth phosphate powders, was registered between 1150°C and 1400°C. Its magnitude was more or less important depending on the synthesis conditions of the powder. In this temperature range, an endothermic peak could appear with a maximum intensity at about 1260°C. It must be noted that the two last thermal peaks at 950°C and 1260°C were not always detected as illustrated in Fig. 2.

High temperature XRD was performed in order to identify the phases responsible for these observed phenomena. Typical XRD diagrams are reported in Fig. 3. The only detected phenomenon was the phase transformation between the rhabdophane-type structure (hexagonal system) and the monazite-type structure (monoclinic system) that was observed from about 600°C for $LaPO_4$ and 650°C for $CePO_4$, temperatures that agree with the literature data [2]. The high temperature monoclinic phase remained stable after cooling to room temperature. It must be aware that anhydrous $LaPO_4$ or $CePO_4$ monoclinic-monazites are different from hydrated $YPO_4 \cdot 2H_2O$ monoclinic-churchite.

These results were confirmed through the characterization of powders heated for 2 h at different temperatures. Figs. 4, 5a and b give the typical XRD diagrams, FTIR spectra and Raman spectra of a calcinated lanthanum phosphate powder. Similar plots could be given for cerium phosphates. The XRD diagrams exhibited the thermostructural change from the hexagonal to the monoclinic structure at the same temperature as that pointed out from high temperature

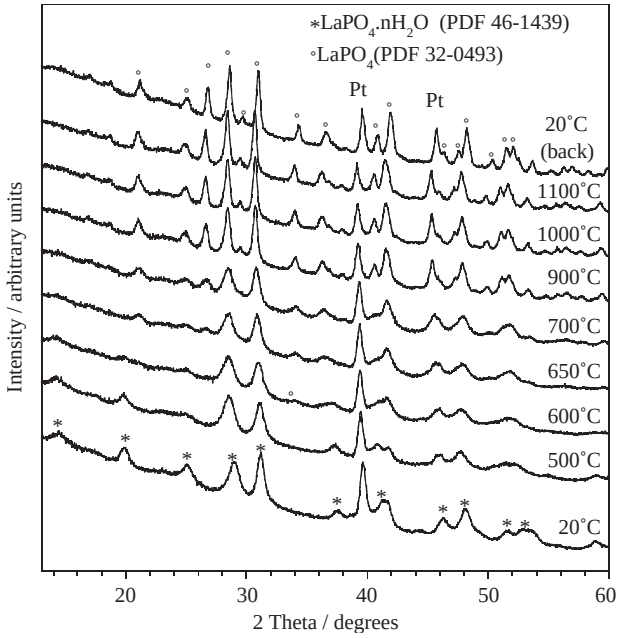

Fig. 3. High temperature XRD diagrams of a lanthanum phosphate precipitate (LaP Tamb).

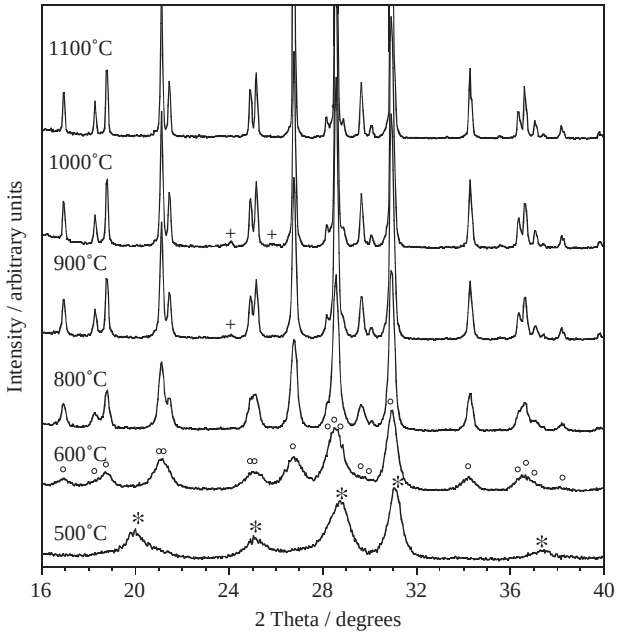

Fig. 4. XRD diagrams of lanthanum phosphate precipitate LaP Tamb after 2 h of calcination at different temperatures. *$LaPO_4 \cdot nH_2O$ (PDF 46-1439); °$LaPO_4$ (PDF 32-0493); +$La(PO_3)_3$ (PDF 33-0717).

XRD. The band at 1631 cm^{-1} on the FTIR spectra was assigned to the hydration water of the hexagonal $LaPO_4 \cdot nH_2O$. This band completely disappeared above 600°C. The other bands were assigned to the phosphate groups [15,16]. For $\theta \leqslant 500$°C, three bands, located at about 542, 570 and 615 cm^{-1}, were clearly observed in the v_4 region of vibration of PO_4 groups. From 600°C,

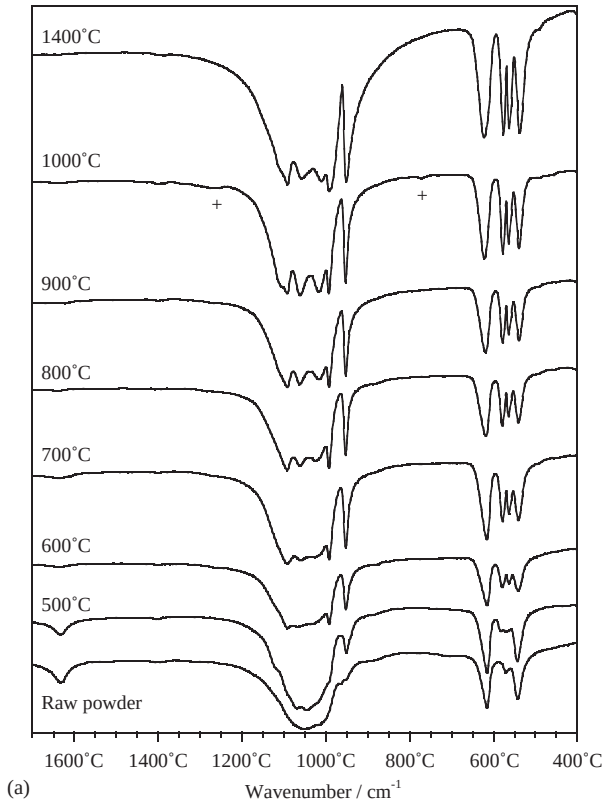

Fig. 5. (a) FTIR spectra of lanthanum phosphate precipitate LaP Tamb after 2 h of calcination at different temperatures (+: trioxophosphate vibration). (b) Raman spectra of lanthanum phosphate precipitate LaP Tamb after 2 h of calcination at different temperatures (+: trioxophosphate vibration).

the middle band seemed split in two vibrations at 565 and 579 cm^{-1}. The same phenomenon was visible in the v_1 region of the Raman spectra with the two bands at 965 and 988 cm^{-1} at high temperature and with a single one at 971 cm^{-1} at low temperature. Though it should also occur in the v_3 region it was not clearly observed on the FTIR spectra because of a low resolution of the different v_3 bands in the domain 990–1100 cm^{-1} at low temperature. In comparison with the low temperature hexagonal structure, the presence of additional bands of phosphate vibrations from 600°C is characteristic of the vibrations of phosphate groups in the monoclinic structure of monazite-type $LaPO_4$ and results from the distortion of the tetrahedral phosphate groups in the nine-fold coordinated La atoms [17].

From these results it can be deduced that the hydration ratio of the hexagonal rhabdophane-type is in agreement with the zeolitic nature of the water in these compounds as already suggested [2,3,18]. This crystalline structure is totally dehydrated below 600°C without structural change, which corresponds to the following equilibrium:

$$[LaPO_4 \cdot nH_2O]_{hexagonal} \rightleftharpoons [LaPO_4]_{hexagonal} + nH_2O^{\uparrow}_{(gas)}. \quad (1)$$

Such a system is divariant, therefore the hydration ratio of the hydrated lanthanum (or cerium) phosphates is variable and depends on both the temperature and the partial pressure of water vapor. The hexagonal to monoclinic transformation is irreversible and begins at 600°C, i.e., after total dehydration of the hexagonal rhabdophane, according to the following reaction:

$$[LaPO_4]_{hexagonal} \rightarrow [LaPO_4]_{monoclinic}. \quad (2)$$

The kinetics of crystallization of the high temperature monoclinic phase appeared low, as indicated by the poor definition of the vibration bands of phosphates in the v_3 region in the domain 990–1100 cm^{-1} of the FTIR spectra of the powders calcinated between 600°C and 900°C. This was confirmed by the XRD diagrams of monoclinic $LaPO_4$ powders calcinated for 2 h in the temperature range 600–1000°C (Fig. 6). The refinement of the diffraction lines was clearly observed with the temperature. This phenomenon was accompanied by a progressive decrease of the mole volume as it can be seen on the dilatometry experiments (Fig. 7). The linear shrinkage recorded up to 600°C for the raw hexagonal hydrated phosphate is due to the contraction of the lattice resulting from the dehydration of the structure. A second shrinkage occurred between 600°C and 900°C and was assigned to the crystallization of the monoclinic anhydrous phosphate formed from the structural change. Similar phenomenon was observed by Terra et al. [19]. The third step of shrinkage at higher temperature was due to the sintering, i.e., the densification

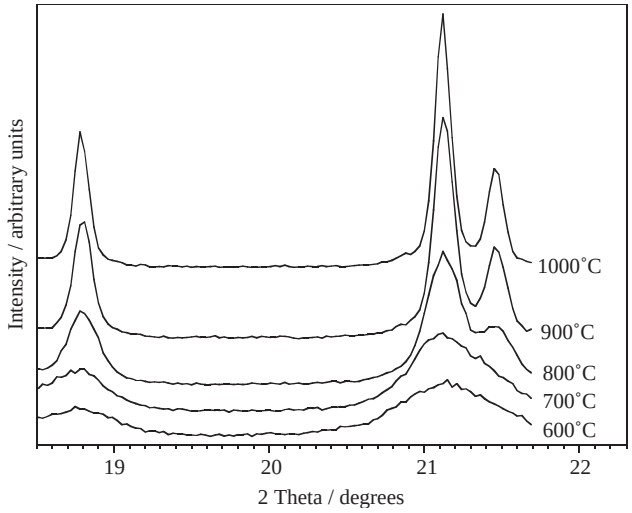

Fig. 6. XRD diagrams of $LaPO_4$ (PDF 32-0493) powders after 2 h of calcination at different temperatures.

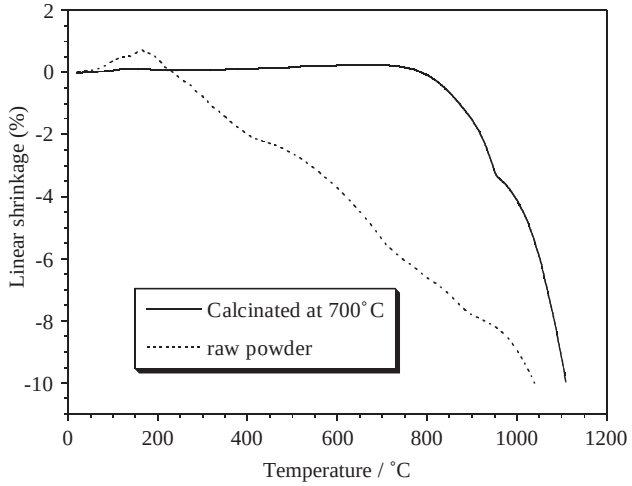

Fig. 7. Linear shrinkage versus the temperature for a lanthanum phosphate powder: raw (hexagonal hydrated form) and calcinated for 2 h at 700°C (monoclinic anhydrous form).

of the material, that will not be discussed in this paper. Assuming that the bulk density of the hexagonal hydrated form is 4.268 and that the bulk density of the monoclinic form is 5.067, the calculated relative contraction of the unit cell volume is of 20.1%. This value agrees with the linear contraction of about 7.5% measured from the ambient temperature up to 900°C for the raw phosphate powder. For the anhydrous monoclinic $LaPO_4$ sample, obtained after an initial calcination of the raw powder for 2 h at 700°C, only the contraction due to the increase of crystallinity of the $LaPO_4$ phase occurred from 700°C up to about 950°C. It must be noted that this contraction remained important with a linear shrinkage of about 3.5%. This may have consequences on the elaboration of rare earth phosphate containing materials.

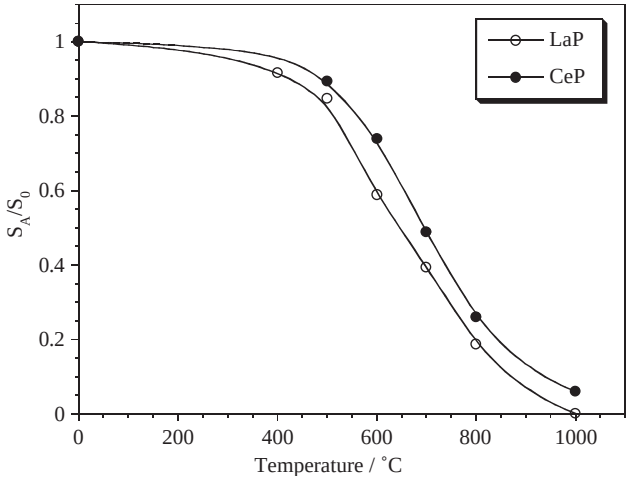

Fig. 8. Normalized surface area of lanthanum and cerium phosphate powders versus the temperature of calcination (2 h holding time).

Morphological changes also occurred during the heating. Fig. 8 gives the plot of the specific surface area of lanthanum and cerium phosphate powders versus the heating temperature (the plot of S_A was normalized according to the specific surface area of the raw powder S_0 given in Table 1). An important decrease was measured between 500°C and 1000°C, which means that particle coalescence occurred in this temperature range. Consequently, though being known as refractory compounds, matter transport can be effective even at a very low temperature, probably through superficial diffusion, mechanism that is often active during the calcination of ceramic oxide powders [20]. The shape of the particles remained unchanged during the calcination, only their size increased. After 2 h at 1000°C the particles were needle-like with a dimension of about 0.5–1 μm length.

Two additional peaks were registered at $2\theta = 24.05°$ and $2\theta = 25.8°$ on the XRD diagram of the lanthanum phosphate powder calcinated at 1000°C (Fig. 4). They appeared at 900°C and disappeared after heating at 1100°C. Both peaks were assigned to polytrioxophosphate $La(PO_3)_3$ (PDF 33-0717) [21] present as secondary phase. According to the preparation and properties of this compound [22], the group $(PO_3)_3$ corresponds to a cyclic polytrioxophosphate. Its vibrations were also detected on the FTIR (Fig. 5a) and Raman (Fig. 5b) spectra of the powder heated at 1000°C with its characteristic vibrations bands at 770 and 1250 cm^{-1} (FTIR) [15,23], and at 684 and 1193 cm^{-1} (Raman) [24], which are the two most intense bands of vibrations of trioxophosphates, identified as $\nu_{symmetric}$ P–O–P and $\nu_{symmetric}$ O–P–O, respectively. It must be noted that, probably due to the very low intensity of PO_3 vibrations and to the presence of intense and broad vibration bands of PO_4 groups in the domain 990–1100 cm^{-1}, there was no evidence for the presence of a band near

$1000\,cm^{-1}$ also mentioned in the literature for cyclic trioxophosphate groups [15,23]. The trioxophosphate vibrations appeared correlatively to the disappearance of the FTIR band at about $875\,cm^{-1}$ assigned to hydrogenphosphate groups that were detected up to 800°C. The same observations could be made from cerium phosphate powders. Considering that the raw powders contain residual H_3PO_4 adsorbed at the particle surface as demonstrated in part I of the study [1], the polytrioxophosphate phase should result from these residuals and their presence would also explain the phenomena observed above 900°C on the TGA-DTA plots. Derivated from different works on the thermal behavior of ammonium dihydrogenphosphate $NH_4H_2PO_4$ mixed with lanthanum phosphate powders [18] or as single solid phase [25], we propose the two following steps to explain the behavior of the powders.

The first step corresponds to the formation of the rare earth polytrioxophosphate (*Re* = La or Ce) from the hydrogenphosphate absorbed at the particle surface of the synthesized precipitates that could be either in the form of residual H_3PO_4 or $NH_4H_2PO_4$ depending on the synthesis conditions:

$$2H_3PO_{4(adsorbed)} + RePO_{4(solid)} \rightarrow Re(PO_3)_{3(s)} + 3H_2O^{\uparrow}_{(g)} \quad (3)$$

or

$$2NH_4H_2PO_{4(ad)} + RePO_{4(s)} \rightarrow Re(PO_3)_{3(s)} + 3H_2O^{\uparrow}_{(g)} + NH^{\uparrow}_{3(g)}. \quad (4)$$

It must be aware that these reactions may proceed according to a mechanism involving several stages that could include the formation at a lower temperature of hydrogen trioxophosphate HPO_3 from the H_3PO_4 or $NH_4H_2PO_4$ initial residuals. Thus, the following mechanisms could also be assessed:

$$H_3PO_{4(ad)} \rightarrow HPO_{3(ad)} + H_2O^{\uparrow}_{(g)} \quad (5)$$

or

$$NH_4H_2PO_{4(ad)} \rightarrow HPO_{3(ad)} + H_2O^{\uparrow}_{(g)} + NH^{\uparrow}_{3(g)}. \quad (6)$$

These transformations are hypothesized because Eqs. (5) and (6) are expected to occur in the temperature range 25–600°C for ammonium dihydrogenphosphate crystals [25], though the behavior of the same compound adsorbed at the surface of a solid particle, as it is the case in our study, may differ. These transformations are hypothesized to occur with the formation of adsorbed HPO_3 because there was no evidence for any solid transformation. The weight loss associated with these reactions could be confused with that due the dehydration of the initial $RePO_4 \cdot nH_2O$ precipitates. This would also mean that the values of the hydration ratios *n* given in Table 1 could be lightly overestimated. Nevertheless, this remark must be moderated because of the very low amount of adsorbed species.

Then, the hydrogen trioxophosphate would react with the rare earth phosphate as

$$2HPO_{3(ad)} + RePO_{4(s)} \rightarrow Re(PO_3)_{3(s)} + H_2O^{\uparrow}_{(g)}. \quad (7)$$

This last step of formation could be associated with the exothermic peak observed on the DTA curves at about 950°C. Considering that the relative amount of the rare earth polytrioxophosphate secondary phase was always below 3 wt%, the weight loss due to water release according to Eq. (7) would be less than 0.15 wt%, which can explain that there was no evidence for a detectable weight loss associated with the formation of $Re(PO_3)_3$ on the TGA plots.

The second step is the decomposition of the polytrioxophosphate phase into a rare earth phosphate between 1050°C and 1350°C:

$$2Re(PO_3)_{3(s)} \rightarrow 2RePO_{4(s)} + P_4O^{\uparrow}_{10(liquid,\ gas)}. \quad (8)$$

A weight loss due to P_4O_{10} gas release from the vaporization of the liquid in this high temperature domain accompanies this incongruent melting of $Re(PO_3)_3$. It corresponds to the weight loss measured in the temperature range 1050–1350°C on the TGA plots and to the endothermic effect that begins at about 1235°C on the DTA curve (see zoom on Fig. 1). This decomposition would be in agreement with the phase diagrams in the system La_2O_3–P_2O_5 established by Park and Kreidler [11] or Kropiwnicka and Znamierowska [12] though they indicate slightly different temperatures for this decomposition, i.e., 1235°C and 1050°C, respectively. The presence of any secondary phase was never detected after calcination at 1400°C and the disappearance of excess phosphorus was also confirmed by the elementary analysis, the heated powders having a *Re*/P mole ratio equal or close to 1. The amount of $Re(PO_3)_3$ was determined from the weight loss between 1000°C and 1400°C according to Eq. (8) (Table 1). As detailed in part I of the study it depended on the synthesis conditions. That explains why the DTA effects may be absent from the plots when the amount is too low for being detected, which is the case of the cerium phosphate powder of Fig. 2 (1.11 wt% against 2.18 wt% for lanthanum phosphate).

Finally, a thermal treatment of the powder at 1400°C is required to insure both the high purity of the powder and the high crystallinity of the monazite-like $LaPO_4$ or $CePO_4$ anhydrous structure. The elimination of the secondary polytrioxophosphate phase that could be present in the intermediate temperature range, and consequently during the sintering of ceramic based rare earth phosphate materials, could also be of prime importance.

3.2. Yttrium phosphates

TGA and DTA plots (Fig. 9) of the amorphous and crystallized hydrated yttrium phosphate precipitates showed that the behavior of these powders were different at low temperature ($\theta < 400°C$) whereas it was similar at high temperature ($\theta > 400°C$). From room temperature to 400°C, the amorphous powder exhibited two different weight losses. The first one, associated with an endothermic effect at about 100°C was due to the release of residual water resulting from the storage conditions, as already observed for lanthanum and cerium phosphate precipitates. The weight loss due to this residual water was all the more important that the powder had a high specific surface area, which explains the particularly high amount in this amorphous yttrium phosphate ($S_0 = 105\,m^2\,g^{-1}$). This water was practically absent in the crystallized precipitate which exhibited small specific surface area ($S_0 \approx 2\,m^2\,g^{-1}$). The second weight loss was observed in both powders. It began at about 200°C for the crystallized powder and it was associated with two endothermic effects. High temperature XRD of this powder (Fig. 10) showed that the transformation from the monoclinic hydrated form $YPO_4 \cdot 2H_2O$ of churchite-type to the anhydrous tetragonal phase YPO_4 of xenotime-type began from 190°C, the low temperature phase having almost totally disappeared at 240°C. Consequently, the two endothermic effects correspond to the release of the hydration water that occurs simultaneously with the phase transformation. This agrees with the following equilibrium:

$$[YPO_4 \cdot 2H_2O]_{monoclinic} \rightleftharpoons [YPO_4]_{tetragonal} + 2H_2O^{\uparrow}_{(g)}. \quad (9)$$

This system has a variance equal to 1, which means that the hydration water of the hydrated form should be constant, i.e., 2 moles, and that this water is coordinated. This result is in agreement with those exposed in part I of the study. As indicated on the XRD diagram after cooling to room temperature, the phase transformation was irreversible in our experimental conditions, only the tetragonal phase was detected.

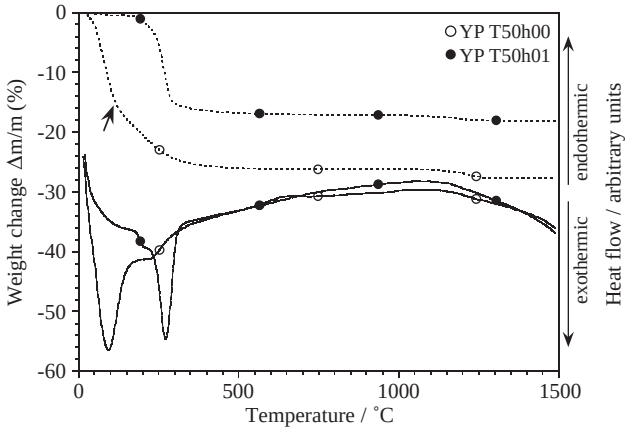

Fig. 9. TGA (dashed line) and DTA of two yttrium phosphate precipitates: without ripening (YP T50h00) and after a 1 h ripening (YP T50h01).

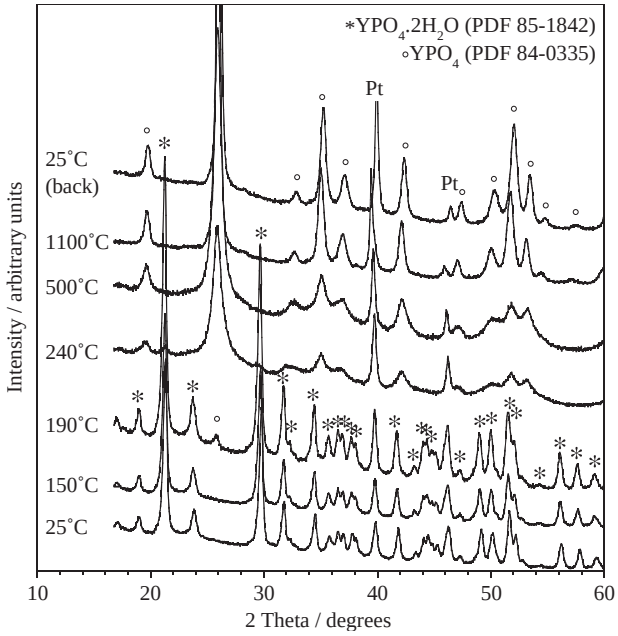

Fig. 10. High temperature XRD diagrams of an yttrium phosphate precipitate (YP T50h01).

The dehydration of the amorphous precipitate was slightly different. Considering that the discontinuity of the weight loss curve (see arrow in Fig. 9) should indicate the beginning of the dehydration of the compound, it seemed to occur from about 100°C in an apparent continuity of the release of the adsorbed residual water. The endothermic effect associated with this dehydration should be in the continuity of that of the release of the adsorbed water as well. A second endothermic peak similar to that registered for the crystallized precipitate was also detected. Fig. 11 shows the XRD diagrams of the amorphous precipitate after different calcination treatments. The small peaks of the minor monoclinic hydrated phase disappeared after 2 h of heating at 300°C, the broad peaks associated with the amorphous phase remained and could be indexed using the same PDF file as the one of the tetragonal anhydrous phase. Then, the refinement of the diffraction peaks indicated a slow increase of the crystallinity of the tetragonal YPO_4 phase with the increase of the heating temperature. These results also agree with the hypothesis that the hydration water was not coordinated in the amorphous compound as stated in part I of the study.

The last weight loss was detected in the range 1100–1300°C (Fig. 9), which was more important for the initially amorphous precipitate than for the crystallized one. As for lanthanum and cerium phosphates this

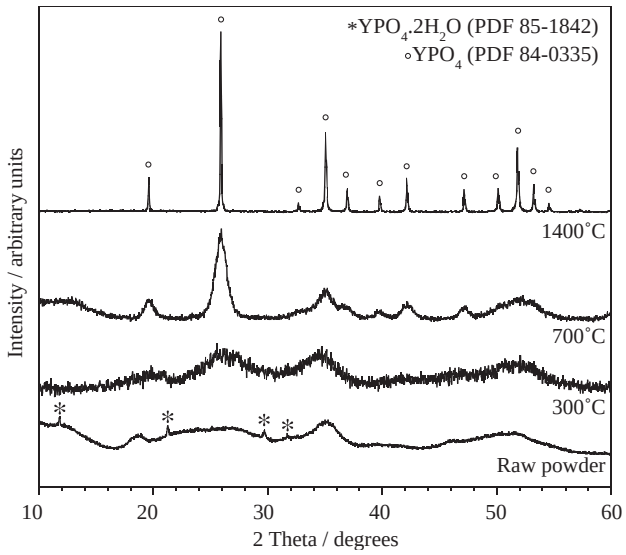

Fig. 11. XRD diagrams of the yttrium phosphate YP T50h00 raw powder and after 2 h of calcination at different temperatures.

weight loss must be associated to the presence of an intermediate yttrium polytrioxophosphate phase formed from H_3PO_4 adsorbed on the surface of the precipitates during the synthesis. The same reaction as Eq. (8) was hypothesized to occur in the temperature range 1100–1300°C:

$$2Y(PO_3)_{3(s)} \rightarrow 2YPO_{4(s)} + P_4O^{\uparrow}_{10(l,\ g)}. \quad (10)$$

Though the phase equilibria in the system Y_2O_3–P_2O_5 described by Agrawal and Hummel [14] indicate a $Y_2P_4O_{13}$ phase in the low temperature of the P_4O_{10} rich-region quite-near YPO_4, the authors specified that because this phase was very difficult to form it can be easily overlooked. Consequently, yttrium polytrioxophosphate is more expected to form. The melting of $Y(PO_3)_3$ appears also controversial. The same authors hypothesized a congruent melting at 1460°C whereas others [26] were in favor of an incongruent melting, as that described through the Eq. (10).

The amount of hypothesized $Y(PO_3)_3$ calculated from these weight losses are given in Table 1. It was much smaller for the crystallized precipitate that exhibited a lower specific surface area than the amorphous compound. This is in agreement with the statement of chemical species initially adsorbed on the surface of the particles. Because present in a very low amount (<1.5 wt%), this yttrium polytrioxophosphate phase could not be directly detected using XRD and the trioxophosphate vibrations were not observed on the FTIR or Raman spectra. The FTIR spectra (Fig. 12) showed the disappearance of the hydrated coordinated water between 200°C and 300°C (bands at 748, 1640 and 1713 cm^{-1}). The Raman spectra (not presented in this paper) were characteristics of the hydrated monoclinic (raw powder) and anhydrous tetragonal yttrium phosphates (calcinated at 1000°C for 2 h). At intermediate temperatures (200°C and 300°C), the spectra exhibited an important background noise that could be associated with a structural disorder that accompanies the phase transformation from the monoclinic to the tetragonal structure.

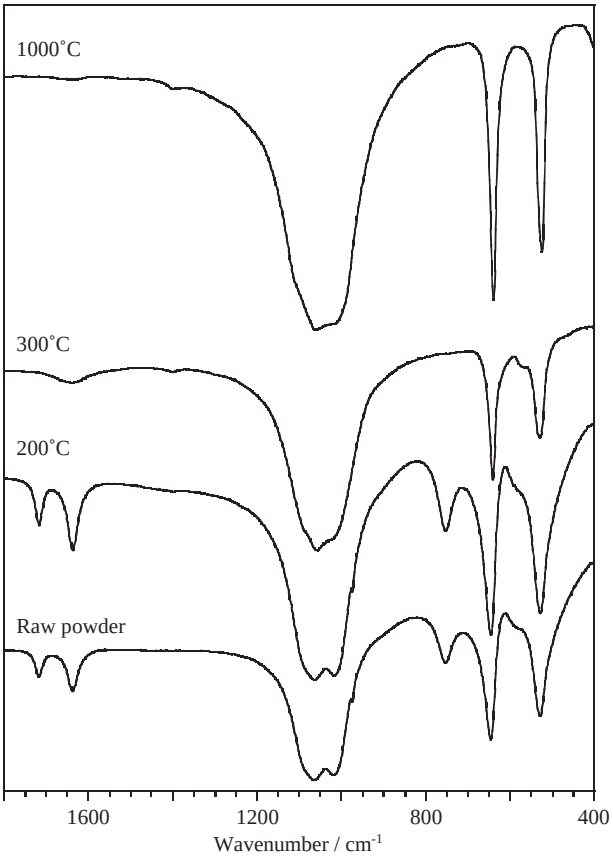

Fig. 12. FTIR spectra of the yttrium phosphate YP T50h01 raw powder and after 2 h of calcination at different temperatures.

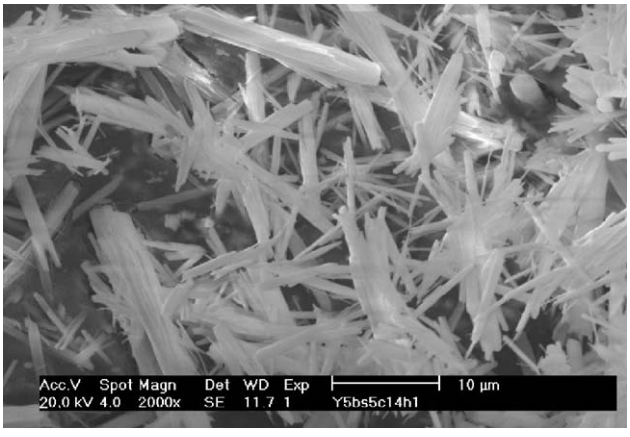

Fig. 13. SEM micrograph of yttrium phosphate powder YP T50h01 after 1 h of calcination at 1400°C.

Compared with the raw precipitates, the heat treatments did not modify the morphology of the powders. The initially amorphous yttrium phosphate remained made of small agglomerated spherical-like particles and the initially crystallized one (YP T50h01) was constituted of needle-like particles, whose length was between 10 and 20 μm (Fig. 13).

4. Conclusion

The thermal behavior of three rare earth phosphate powders synthesized using a wet process was investigated. Similar behavior was found for lanthanum and cerium phosphates. The dehydration of the hexagonal hydrated structure occurred according to a divariant equilibrium without any phase change. The transformation from the hexagonal to the monoclinic structure of monazite-type (La or Ce)PO_4 began at about 600°C and it was irreversible. The crystallinity of this last phase was found to increase slowly with the temperature and it was completed only above 900°C.

On the opposite, the dehydration equilibrium of the yttrium phosphate of monoclinic structure agreed with a variance equal to 1 and it was accompanied by the phase change from the monoclinic hydrated structure into the anhydrous tetragonal structure of xenotime-type YPO_4.

Whatever the composition and synthesis conditions considered, a secondary minor polytrioxophosphate phase $Re(PO_3)_3$ with Re = La, Ce or Y formed from about 950°C to disappear above 1350°C. This phase, though often undetectable using conventional characterization techniques when present in a very low amount, may influence the high temperature sintering (densification ability of the material, grain growth, …) and the resulting properties of the ceramics. This will be exposed in a forthcoming paper devoted to the processing and mechanical properties of dense rare earth phosphate ceramics.

References

[1] S. Lucas, E. Champion, D. Bregiroux, D. Bernache-Assollant, F. Audubert, J. Solid State Chem., to be published.
[2] R.G. Jonasson, E.R. Vance, Thermochim. Acta 108 (1986) 65–72.
[3] Y. Hikichi, J. Sasaki, S. Susuki, K. Murayama, M. Miyamoto, J. Am. Ceram. Soc. 71 (1988) c354–c355.
[4] H. Assaaoudi, A. Ennaciri, A. Rulmont, M. Harcharras, Phase Transitions 72 (2000) 1–13.
[5] W. Min, K. Daimon, T. Ota, T. Matsubara, Y. Hikichi, Mater. Res. Bull. 5 (2000) 2199–2205.
[6] Y. Hikichi, T. Sasaki, K. Murayama, T. Nomura, M. Miyamoto, J. Am. Ceram. Soc. 72 (1989) 1073–1076.
[7] Y. Hikichi, T. Nomura, J. Am. Ceram. Soc. 70 (1987) C252–C253.
[8] J.J. Serra, J. Coutures, A. Rouanet, High Temp. High Pres. 8 (1976) 337–341.
[9] A. Rouanet, J.J. Serra, K. Allaf, J. Coutures, H. Dexpert, Rev. Inter. Hautes Tempér. Réfract. 16 (1979) 437–443.
[10] A. Rouanet, J.J. Serra, K. Allaf, V.P. Orlosvkii, Inorg. Mater. 17 (1981) 76–81.
[11] H.D. Park, E.R. Kreidler, J. Am. Ceram. Soc. 67 (1984) 23–26.
[12] J. Kropiwnicka, T. Znamierowska, Polish J. Chem. 62 (1988) 587–594.
[13] M.S. Wong, E.R. Kreidler, J. Am. Ceram. Soc. 70 (1987) 396–399.
[14] D. Agrawal, F.A. Hummel, J. Electrochem. Soc. 127 (1980) 1550–1554.
[15] A. Rulmont, R. Cahay, M. Liegois-Duyckaerts, P. Tarte, Eur. J. Solid State Inorg. Chem. 28 (1991) 207–219.
[16] G.M. Begun, G.W. Beall, L.A. Boatner, W.J. Gregor, J. Raman Spectrosc. 11 (1981) 273–278.
[17] D.F. Mullica, W.O. Milligan, D.W. Grossie, L.A. Boatner, Inorg. Chim. Acta 95 (1984) 231–236.
[18] M. Junker, Thesis, ENSM St Etienne and INP Grenoble, 1995.
[19] O. Terra, N. Clavier, N. Dacheux, R. Podor, New J. Chem. 27 (2003) 957–967.
[20] D. Bernache-Assollant, A. Ababou, E. Champion, M. Heughebaert, J. Eur. Ceram. Soc. 23 (2003) 229–241.
[21] I.L. Botto, E.J. Baran, J. Appl. Cryst. 12 (1979) 257–258.
[22] Y. Gushikem, E. Giesbretcht, O.A. Serra, J. Inorg. Nucl. Chem. 34 (1972) 2179–2187.
[23] D.E.C. Corbridge, E.J. Lowe, J. Chem. Soc. (1954) 493–502.
[24] G.M. Begun, C.E. Bamberger, J. Raman Spectrosc. 13 (1982) 284–289.
[25] A. Abdel-Kader, A.A. Ammar, S.I. Saleh, Thermochim. Acta 176 (1991) 293–304.
[26] M. Bagieu-Beucher, T.Q. Duc, Bull. Soc. Fr. Mineral. Crystallogr. 93 (1970) 505.